Insertion of the Al Atom into Alkyl Ethers: Semiempirical SCF MO and Matrix Isolation ESR Study

Paul H. Kasai

IBM Research Division, Almaden Research Center, San Jose, California 95120-6099

Received: August 10, 2001; In Final Form: October 23, 2001

The insertion process of the Al atom into trimethylene oxide (TMO) and that into dimethyl ether (DME) were examined by a semiempirical SCF molecular orbital method (AM1) and by matrix isolation ESR spectroscopy. The MO study revealed the three step process: (1) an approach of the Al atom toward the ethereal oxygen along the C_{2v} axis of the molecule driven by a favorable overlap between the aluminum SOMO (the $3p_z$ orbital) and the LUMO of the molecule of A_1 symmetry, (2) formation of the Al−O dative bond with concurrent scission of one of the C−O bonds, and (3) completion of the process by the three-electron bonding scheme between the unpaired electron on the alkyl terminus and the lone pair electrons on Al. The MO study also revealed that the process would be spontaneous for the Al/TMO system, but for the Al/DME system, there existed a barrier of ∼8 kcal/mol for the onset of the methyl group cleavage from the dative complex $Al:O(CH_3)_2$. The MO study also revealed that, in the Al/DME case, the insertion product $CH_3-Al-O-CH_3$ of the cis conformation was initially formed but it might readily convert to the more stable trans form. The ESR study revealed that the Al atom insertion into TMO occurred spontaneously. Well-resolved spectra of the expected insertion radical $\overset{\frown}{CH_2-Al-O-CH_2-CH_2}$ were observed. In the case of DME, the ESR study revealed the presence of both the intermediate dative complex and the final insertion product in the as-prepared matrix. When the matrix was subsequently irradiated with red light ($\lambda = 700 \pm 50$ nm), the dative complex resumed the process and converted to the insertion product. The insertion radicals of both the cis and trans forms were observed in the argon system, but only the more stable trans radical was observed in the neon system.

Introduction

Many matrix isolation studies have shown that the Al atom has a propensity to insert itself into heteroatomic bonds. Hauge et al. reported on spontaneous formation of divalent alumino radicals H−Al−OH upon co-condensation of Al atoms and H_2O in argon matrixes.[1] The formation of the insertion product was established by an IR study of the matrixes. Knight et al. observed and analyzed later the ESR spectra of H−Al−OH generated in neon and argon matrixes.[2] Howard et al. reported on formation of the corresponding insertion product $H-Al-NH_2$ upon co-condensation of Al atoms and NH_3 in adamantane matrixes at 77 K.[3] Chenier et al. reported on the ESR spectra of insertion products, R−Al−O−R, generated upon co-condensation of Al atoms and various alkyl ethers in adamantane matrixes.[4] More recently, a study at our laboratory revealed formation of H−Al−Cl upon co-condensation of Al atoms and HCl molecules in argon matrixes.[5] In each of these reports, based on the fact that the reaction occurred in a cryogenic environment, it was asserted that Al atoms in the ground state reacted spontaneously to form the observed insertion radicals. Using ab initio molecular orbital methods, Sakai examined the insertion reaction of the Al atom into H−X bond (X = F, O, N, C, S, and P)[6] and those into H_2O and dimethyl ether molecules.[7] He concluded that, in each of these cases, the insertion process commenced with an electron transfer from the Al atom into the antibonding orbital of the subject bond. More recently, Fäugström et al. examined, on the basis of the density functional theory, the potential energy surface of the reaction between the Al atom and dimethyl ether.[8] The study predicted the reaction passage effecting the Al insertion into one of the C−H bonds, as well as the passage effecting the insertion into one of the C−O bonds. The most stable products were the cis and trans conformers of the latter reaction, $CH_3-Al-O-CH_3$. The reaction processes were not discussed in terms of electron flow(s), however.

The efficacy of a semiempirical SCF molecular orbital method (e.g., AM1) in elucidating the reaction process between a paramagnetic atom and a small molecule has been demonstrated in our recent study of the reaction between Li atoms and HX (X = F, Cl) molecules.[9] The MO study predicted that the Li atom would approach the H−Cl (or F) molecule spontaneously driven by the three-electron bonding scheme between the Li unpaired electron and the lone pair electrons of the halogen atom. In the case of HCl, when the orbital level of the SOMO (singly occupied molecular orbital) of the reacting system (given by the antibonding combination of the Li 2s orbital and the Cl 3p orbital) becomes higher than that of the vacant antibonding orbital of the H−Cl sector, the unpaired electron migrates into the HCl moiety. The final structure of the Li:HCl complex would be that of an elongated H−Cl sided by the Li atom bearing a substantial positive charge. In the case of H−F, the corresponding level crossing does not occur. The structure of the Li:HF complex would be that given by the initial three-electron bonding scheme only; the Li atom docks onto the F atom and bears a negative charge. An ESR study of the Al/HX (X = Cl and F)/Argon system clearly revealed spontaneous formation

10.1021/jp013133v CCC: $22.00 © 2002 American Chemical Society
Published on Web 11/29/2001

of these complexes having structures in total accord with those predicted by the theory.

To gain a clearer understanding of the Al atom's propensity for insertion, we have presently examined, first by a semi-empirical SCF molecular orbital method (AM1) and then by matrix isolation ESR spectroscopy, the reaction between the Al atom and the TMO (trimethylene oxide) molecule and that between the Al atom and DME (dimethyl ether) molecule. The molecular orbital study has revealed that the insertion of the Al atom ($3s^23p^1$) into an alkyl ether would occur in three steps: (1) spontaneous approach of the Al atom toward the ethereal oxygen driven by migration of the Al unpaired electron into the LUMO (the lowest unoccupied MO) of the ether, (2) formation of the Al−O bond with concurrent cleavage of one of the C−O bonds, and (3) completion of the insertion process by the three-electron bonding scheme between the unpaired electron of the alkyl radical (generated in step 2) and the lone pair electrons on the Al atom. The unpaired electron is transferred back to the Al atom in the final step. The matrix isolation ESR study clearly revealed the formation of the insertion radicals, $\overbrace{CH_2-Al-O-CH_2-CH_2}$ and $CH_3-Al-O-CH_3$. Most interestingly, in the case of Al/DME system, a metastable intermediate species $Al{:}O(CH_3)_2$ was predicted and observed, and the final insertion products $CH_3-Al-O-CH_3$ of both the cis and trans forms were recognized.

Experimental and Computational Methods

A liquid helium cryostat that would allow trapping of vaporized metal atoms in an argon matrix and examination of the resulting matrix by ESR has been described earlier.[10] In the present series of experiments, Al atoms were vaporized from a resistively heated (∼1400 °C) tantalum tube and were trapped in argon or neon matrixes containing TMO or DME (1−2%). All the ESR spectra were obtained while the matrix was maintained at ∼4 K. The spectrometer frequency locked to the sample cavity was 9.428 GHz. For photoirradiation of the resulting matrix, a high-pressure Xe/Hg lamp (Oriel 1 kW) fitted with a water filter and a broad band interference filter of appropriate choice was used. DME (dimethyl ether) and TMO (trimethylene oxide) were obtained from Aldrich Chemical.

For examination of the viable reaction passage by the semiempirical SCF molecular orbital method, the AM1 program implemented in HyperChem was used.[11] The TMO or DME molecule was first geometry optimized and the Al atom was placed ∼3 Å away; the total system was then geometry optimized following the energy surface trough (the steepest descent). For simulation of ESR spectra, a Fortran program written and described earlier[12] was modified for execution on an IBM-compatible PC using Absoft compiler.[13]

Computational Results

As stated above, our recent study of the reaction between the Li atom and the H−Cl molecule has revealed that the reaction commences with the attraction arising from the three-electron bonding scheme between the unpaired electron of the Li atom and the lone pair electrons of the halogen atom and, when the energy level of the SOMO of the reacting system (given by the antibonding combination of the Li valence orbital and the halogen p orbital) crosses the level of the antibonding orbital of the H−Cl moiety, the unpaired electron migrates from the former to the latter.[9] In a separate, earlier matrix isolation ESR study, it has been shown that when an electron is added to TMO, the resulting anion has the ring-opened structure as shown below.[14]

On the basis of these results, one may postulate that the insertion of an Al atom into the TMO ring occurs as follows.

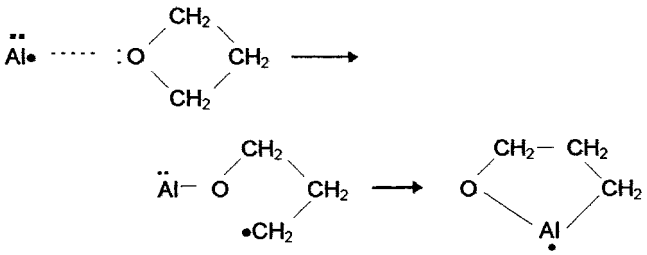

The ring closure, the completion of the insertion process, is driven by the three-electron bonding scheme between the unpaired electron on the alkyl terminus and the lone pair electrons on the Al atom.

Examination of the reaction between the Al atom and TMO molecule by the SCF semiempirical molecular orbital method (AM1) revealed the reaction passage(s) depicted in Figure 1. For each stage, the positions of the atoms, bonds, and the isosurface contour rendering of the SOMO are shown. It is revealed that the Al atom approaches the ethereal oxygen of TMO along its C_{2v} symmetry axis. The driving force, however, is not the envisaged three-electron bonding scheme, but that of a simple overlap between the SOMO of the reacting system (the Al p_z orbital of A_1 symmetry) and the LUMO of the reacting system (the LUMO of TMO of A_1 symmetry). As the Al−O bond is formed, the unpaired electron migrates further, and eventually the ring ruptures (the stage B → C in Figure 1). Subsequently, in stage C, the three-electron bonding reaction does take place between the unpaired electron on the alkyl terminus and the lone pair electrons on the Al atom, thus leading to the insertion product (stage D). The entire process is spontaneous (exothermic throughout), and the heat of insertion is ∼95 kcal/mol.

A similar reaction process predicted for the insertion of the Al atom into the DME molecule is shown in Figure 2. Here a slight (perhaps insignificant) barrier is indicated before reaching stage C which is 21 kcal/mol more stable than the starting separated system. Of more interest is the indicated presence of a barrier of ∼8 kcal/mol for the onset of the methyl radical cleavage. In actual calculation, the oxygen atom in the metastable dative complex C was moved slightly upward (ca. 0.1 Å), mimicking the C−O−C antisymmetric vibration. The methyl group then cleaved spontaneously (stage D), and the insertion product was subsequently formed via the three-electron bonding scheme (stage E). The insertion product thus formed was always in the cis conformation. A further perusal showed that the insertion product of the trans form, stage F, was equally (or perhaps slightly more) stable, and there existed a slight barrier (∼4 kcal/mol) for the cis−trans conversion as indicated.

As stated above, in both the Al/TMO and Al/DME cases, the reaction is initially driven by the migration of the unpaired electron from the Al p_z orbital of the A_1 symmetry into the LUMO of TMO (or DME) of the same symmetry. It should be emphasized that this electron flow occurrs only when the Al atom approaches the ethereal oxygen precisely along the C_{2v}

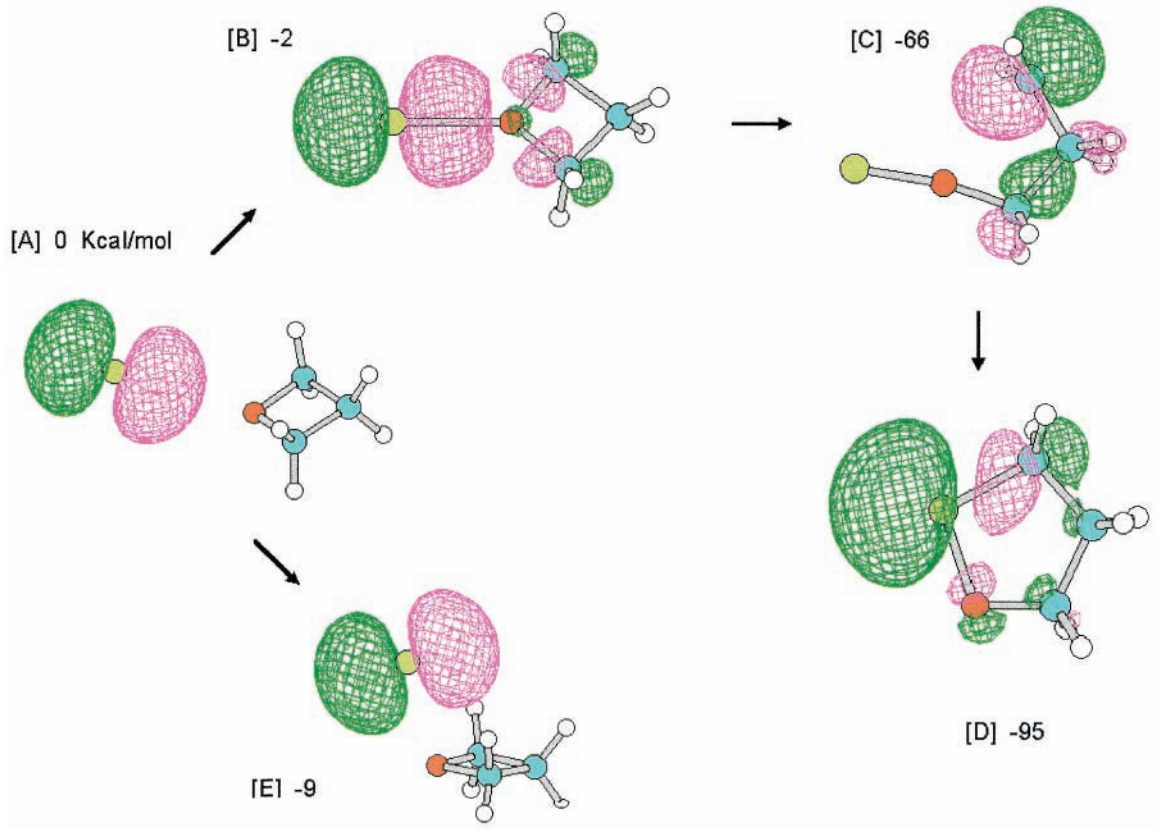

Figure 1. Insertion process of the Al atom into trimethylene oxide revealed by the SCF MO (AM1) method. The energy level (relative to the starting separated system) and the isosurface contour rendering of the SOMO at each stage are shown.

symmetry axis. If it approaches off the symmetry axis, the three-electron bonding scheme becomes dominant, and the unpaired electron in the antibonding combination (of the reacting orbitals) moves immediately into the Al p_x orbital of the B_2 symmetry (retaining the notation of the symmetric structure).

Sakai found, in his ab initio calculation, the association complex of the B_2 symmetry with the Al−O distance of ∼2.3 Å and the formation energy of 9 kcal/mol. He concluded that the Al atom insertion into the C−O bond occurred when the unpaired electron in the Al p_x orbital of the B_2 symmetry migrated into the C−O−C antibonding orbital of DME of the same symmetry.[7] Fäugström et al. also found, in their study by the density functional method, a stationary state of the Al−DME system with the geometric features identical to the association complex of the B_2 symmetry discussed by Sakai. They did not discuss the electronic symmetrry of the complex, nor the electron flow involved, but asserted that this stationary state lead to the Al insertion into the C−O bond. The Al−DME dative complex given at the stage C in Figure 2 is at odds with the stationary states found in the earlier ab initio studies. It is much more stable (−21 kcal/mol) with the Al−O bond distance of ∼1.8 Å, and has the A_1 electronic symmetry. The isosurface contour renderings of the LUMO's (A_1) and the C−O−C antibonding orbitals of the B_2 symmetry yielded by the AM1 method for the isolated TMO and DME molecules are shown in Figure 3. In both cases, the C−O−C antibonding orbital of the B_2 symmetry is the molecular orbital of the highest energy level yielded by the calculation and is several electrovolts above the LUMO. The reaction process resulting from an electron flow from the HOMO into the LUMO of the reacting system, if attainable, is more likely to occur than that requiring a flow into the highest unoccupied MO. In the reaction energy surface study by the AM1 method, when the three-electron mechanism dominates (due to initial disposition of the Al atom), it often leads to the formation of a weak association complex at the energy level of −9 kcal/mol with its unpaired electron in the Al p orbital perpendicular to the Al−O internuclear direction (stage E in Figure 1 and stage G in Figure 2). No electron migration of consequence occurred from this stage, however.

Experimental Result: The Al/TMO System

From the Al−ether insertion products generated in adamantane matrixes at 77 K, Chenier et al. observed ESR spectra comprising a sextet with successive spacings of ∼300 G.[4] The sextet splitting is due to the hfc (hyperfine coupling) interaction with the ^{27}Al nucleus ($I = {}^5/_2$, natural abundance = 100%). The observed large and essentially isotropic Al hfc tensor is consistent with the unpaired electron residing mainly in a sp hybridized orbital of the Al atom. For similar Al insertion radicals generated in rare gas matrixes and examined at ∼4 K, ESR spectra of higher resolution revealing an axial symmetry of the Al hfc tensor are expected.

Figure 4a shows the ESR spectrum observed from the Al/TMO(2%)/argon system. The sextet pattern due to an Al hfc tensor of axial symmetry was readily recognized as indicated. The multiplets observed in the central region (indicated by the bracket) are signals due to isolated Al atoms and TMO anions (with the ring-opened structure). The ESR spectra of aluminum atoms isolated in rare gas matrixes had been analyzed by Ammeter et al.[15] The TMO anions are believed to have been generated during deposition via collision in flight and/or in a fluid surface layer. The second, satellite-like sextet of less intensity with the Al hfc tensor slightly reduced from that of the main sextet is also recognized (indicated by slanted arrows). We (tentatively) assigned the main sextet to the insertion

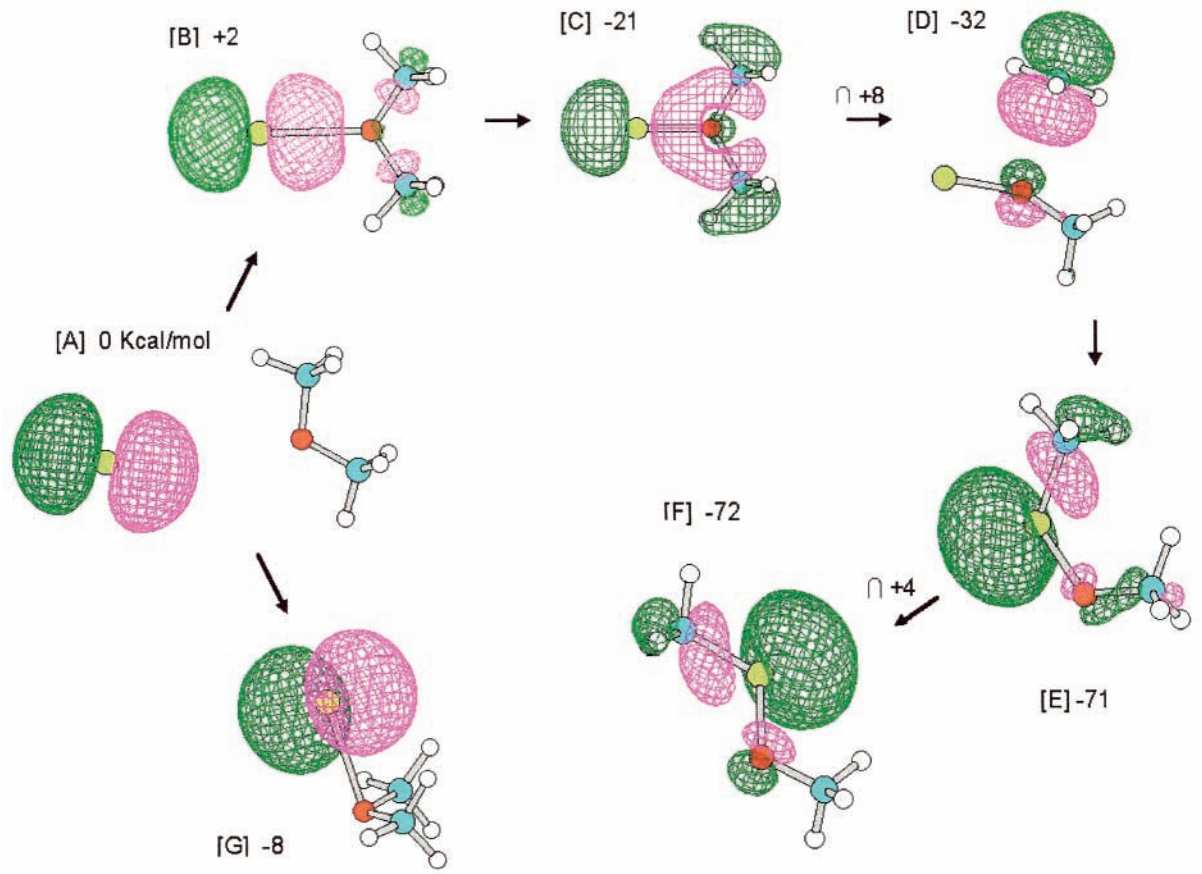

Figure 2. Insertion process of the Al atom into dimethyl ether revealed by the SCF MO (AM1) method. The energy level (relative to the starting separated system) and the isosurface contour rendering of the SOMO at each stage are shown.

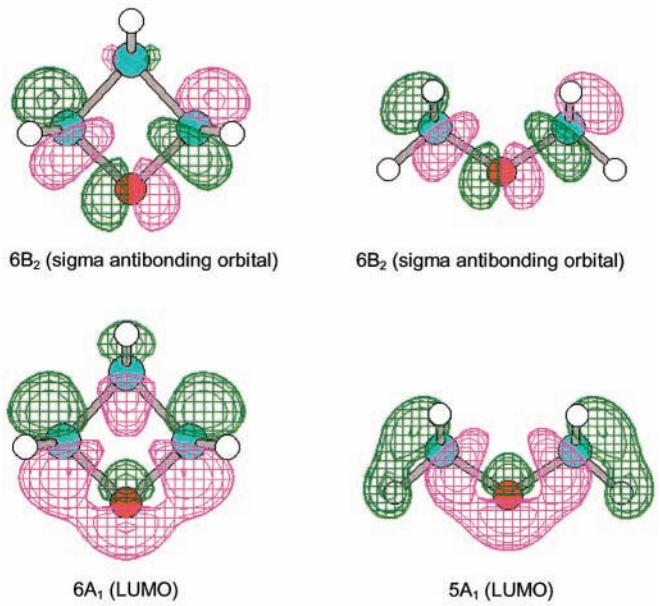

Figure 3. Isosurface contour renderings of the LUMO of A_1 symmetry and the antibonding σ orbital of B_2 symmetry given by the AM1 method for the trimethylene oxide (left) and dimethyl ether (right) molecules.

product, Al−TMO, of stage D in Figure 1, and the satellite sextet to the primary insertion radical datively complexed with the second TMO molecule. When the experiment was repeated with the TMO concentration reduced from 2% to 1%, the intensity of the signals due to isolated Al atoms relative to the main sextet increased by the factor of 2, and that of the satellite sextet decreased by the factor of 2.

TABLE 1: *g* Tensors and Al Hyperfine Coupling Tensors of Al−TMO and Al−DME Insertion Radicals and Al:DME Dative Complex Observed in Argon and Neon Matrixes

insertion radical	matrix	Al hfc tensor (in gauss)	*g* tensor
Al−TMO	argon	380/320/320	2.000/2.000/1.997[a]
Al−TMO	neon	376/316/316	2.000/2.000/1.997
Al−DME (cis)	argon	409/357/357	2.000/2.000/1.997[a]
Al−DME (trans)	argon	357/305/305	2.000/2.000/1.997[a]
Al−DME (trans)	neon	346/295/295	2.000/2.000/1.997[a]
Al:DME[b]	neon	43.0/25.4/26.4	2.0008/1.9952/1.9879
Al−DME[c]	adamantane	358	2.0004

[a] g_3 was assumed to be the same as that of Al−TMO determined in a neon matrix. [b] The metastable dative complex (stage C in Figure 2). [c] The data reported by Chenier el at. (ref 4).

The *g* tensor and Al hfc tensor of the insertion product, Al−TMO, determined from the spectrum is shown in Table 1. For analysis of the ESR spectral pattern characterized by a large Al hfc tensor, the exact solution of the spin Hamiltonian based on the continued fraction technique was used.[16] Figure 4b shows the computer simulated pattern based on the *g* tensor and the Al hfc tensor thus determined.

Figure 5 shows the ESR spectrum observed from the Al/TMO(1%)/neon system. The spectral pattern essentially identical to that observed from the argon system is recognized. The individual spectral features are sharper, reflecting a better annealing achieved in a neon matrix, and the signals due to isolated Al atoms are absent. The spectral pattern due to TMO anions of ring opened structure was thus observed without interference, as shown. The *g* tensor and the Al hfc tensor of the Al−TMO insertion radical generated in the neon matrix are also included in Table 1.

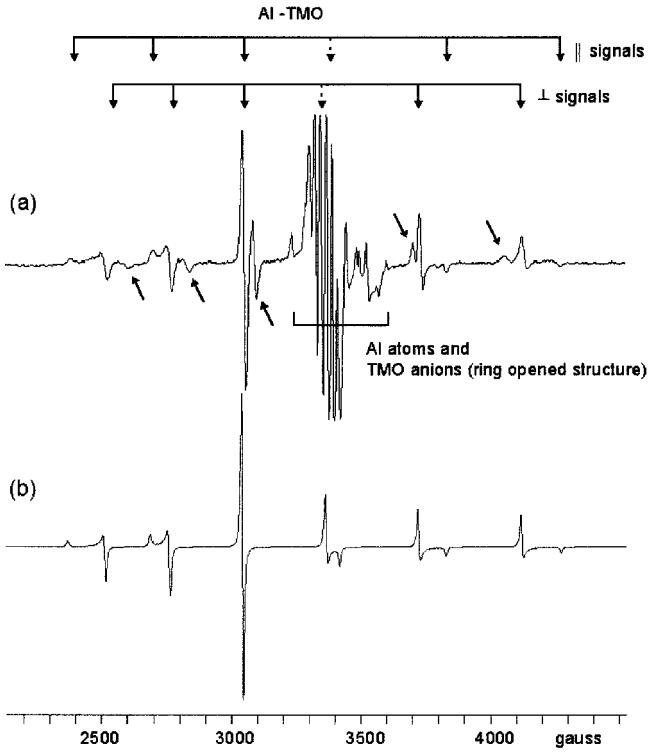

Figure 4. (a) ESR spectrum observed from the Al/TMO(2%)/argon system. The spectral pattern due to the insertion product Al−TMO with an axially symmetric Al hfc tensor was recognized as indicated. The satellite (indicated by slant arrows) is assigned to insertion radicals complexed with the second TMO molecule. (b) The spectrum of the insertion radical simulated based on the g and Al hfc tensors given in Table 1.

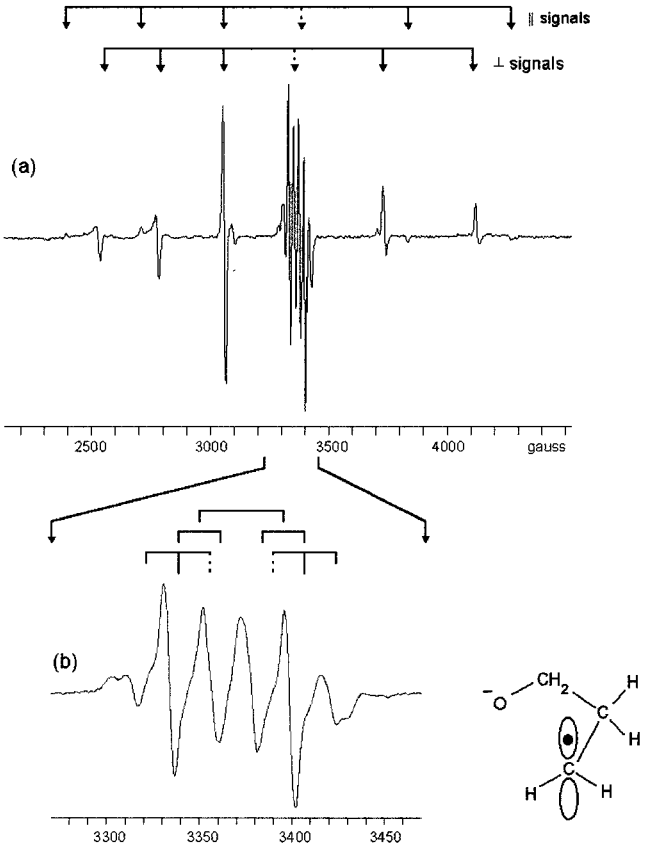

Figure 5. (a) ESR spectrum observed from the Al/TMO(1%)/neon system. The spectrum due to the insertion product with an axially symmetric Al hfc tensor is indicated. (b) The central section observed in an expanded scale. The signals are due to TMO anions of ring-ruptured form; the indicated doublet-of-doublet-of-triplet pattern arises from the two nonequivalent β protons and the two α protons undergoing rapid exchange (see ref 13).

It is intriguing that for these Al−TMO insertion radicals, the effect of the anisotropy of the Al hfc tensor essentially vanishes for the third Al hyperfine component ($m_I = {}^1/_2$). It was thus hoped that the hf structure due to the protons of the adjacent methylene group might be resolved there in the neon system. No structure was apparent when the particular hf component was examined in an expanded scale in the usual derivative pattern. Most gratifyingly, however, when the component was examined in the second derivative form, a pattern akin to that expected from the hfc interaction with two equivalent protons clearly emerged (Figure 6a). Figure 6b is the third hf component simulated based on the g and the Al hfc tensor determined earlier and the hfc interaction of 3.5 G (the triplet like splitting observed in Figure 6a) with two protons. The variance between the observed and simulated pattern was thought due to an anisotropy of the g tensor. It has been shown that for a radical with a well separated ground state $|0\rangle$, the deviation of the g tensor from the spin only value g_e is given as follows:[17]

$$g_i - g_e = -2\lambda \sum_n \frac{\langle 0|L_i|n\rangle\langle n|L_i|0\rangle}{E_n - E_0} \qquad (1)$$

Here i (= x, y, z) represents a principal axis of the g tensor, L_i the orbital angular momentum operator, and λ the one-electron spin−orbit coupling constant. The summation is to be performed for all the excited states $|n\rangle$. As seen in Figure 1, stage D, the SOMO of the insertion product is mostly a sp hybridized orbital of the Al atom. Thus, it may be given as $\Phi_0 \cong a\phi_{Al}(3s) + b\phi_{Al}(3p_z) + c\phi_{TMO}$, where the last term represents the part involving the neighboring atoms. The Al hfc tensor would be axially symmetric about the z axis. The analysis of the Al hfc tensor determined for the insertion radical Al−TMO generated in a neon matrix yielded $a^2 \cong 0.25$ and $b^2 \cong 0.67$ (vide infra). Of all the possible excited states, that which would have nontrivial contribution in eq 1 is the vacant Al p orbital perpendicular to the molecular plane. We hence predict that the principal g value perpendicular to the symmetry axis and parallel to the molecular plane would be less than g_e. Setting $\lambda = 0.0093$ eV (the spin−orbit coupling constant of the Al atom estimated from the fine structure spacing of the atomic spectrum[18]) and $E_n - E_0 = 5$ eV (estimated from the MO result) and using the orbital reduction factor estimated above (0.67), one obtains $g_i - g_e \cong 0.003$. In computing the pattern shown in Figure 6b, it was assumed that $g_{\|} = g_{\perp} = 2.000$. Figure 6c shows the pattern obtained when one of the $g_{\perp}$ values was changed to 1.997.

Experimental Result: the Al/DME system

Figure 7a shows the ESR spectrum observed from the Al/DME(1%)/argon system. In contrast to the Al/TMO system, there are two sets of sextets arising from two significantly different Al hfc tensors of axial symmetry. As stated earlier, the computational study predicted the possible presence of the Al insertion product into DME in both the cis and trans forms. The SOMO's of these products given by the theory are such that the unpaired electron density in the Al 3s orbital would be ~10% smaller for the trans form. Accordingly, the two sets of sextets were assigned to the cis and trans forms of the insertion radicals Al−DME as indicated. The g tensors and the Al hfc tensors determined respectively are included in Table 1. Figure

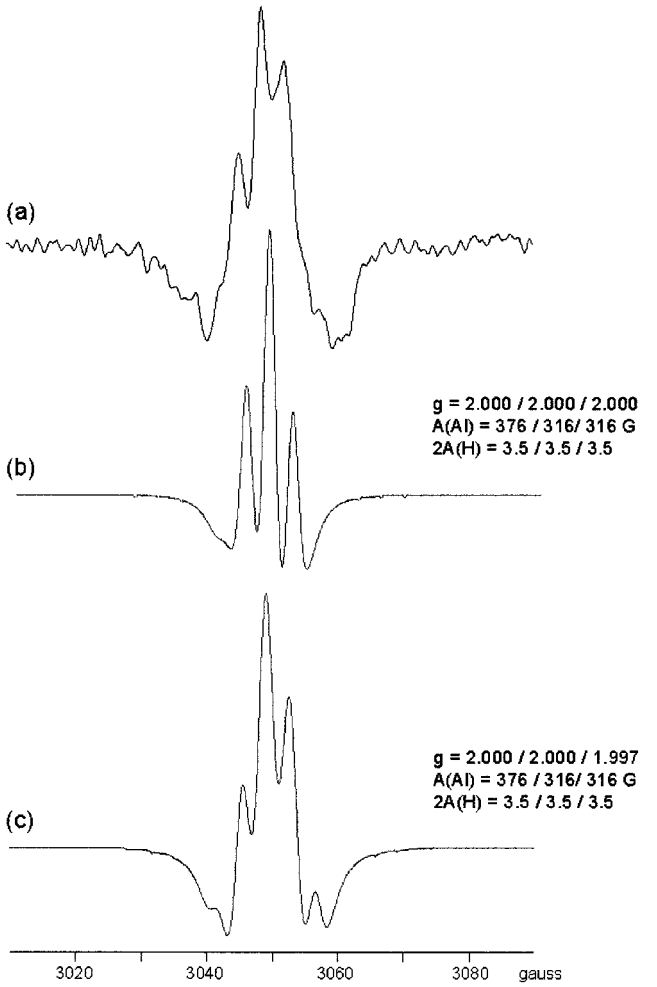

Figure 6. (a) Third Al hf component of the insertion radical of Figure 5a shown expanded in the second derivative form. (b) A simulated pattern based on the isotropic *g* tensor and the Al and proton hfc tensors indicated. (c) A similarly simulated pattern changing one of the $g_{\perp}$'s from 2.000 to 1.997 (see text).

7b is a computer simulated pattern based on these tensors and the abundance ratio of $^1/_3$ for the cis and trans forms. As shown in Figure 2, the MO study predicted a spontaneous insertion process leading to the cis form, a rather marginal energy difference between the cis and trans form, and a barrier of several kilocalories per mole for the conversion. The fact that the trans form is more abundant indicates that the trans form is clearly more stable. When the matrix was deposited with simultaneous irradiation with red light ($\lambda = 700 \pm 50$ nm.), the intensity of the "cis" sextet became ~1/10 of that of the "trans" sextet.

Unlike TMO, DME does not form anion radicals. The signals in the central region (indicated by the bracket in Figure 7a) were expected to be those of isolated Al atoms and the fourth hf components of the insertion radicals. Figure 8a shows this region observed in an expanded scale. In addition to signals due to inadvertently formed methyl radicals and those of isolated Al atoms, several signals (indicated by arrows) were observed which did not belong to the fourth hf component of either the cis or trans insertion radical. Most interestingly, when the matrix was irradiated with red light ($\lambda = 700 \pm 50$ nm) for 20 min, those signals decayed drastically (Figure 8b). The photo labile signals are believed due to the dative complex (stage C in Figure 2) of a local minimum. The small but highly anisotropic Al hfc tensor implied by these signals is consistent with the SOMO, predicted by the MO study, consisting mainly of the Al 3p and

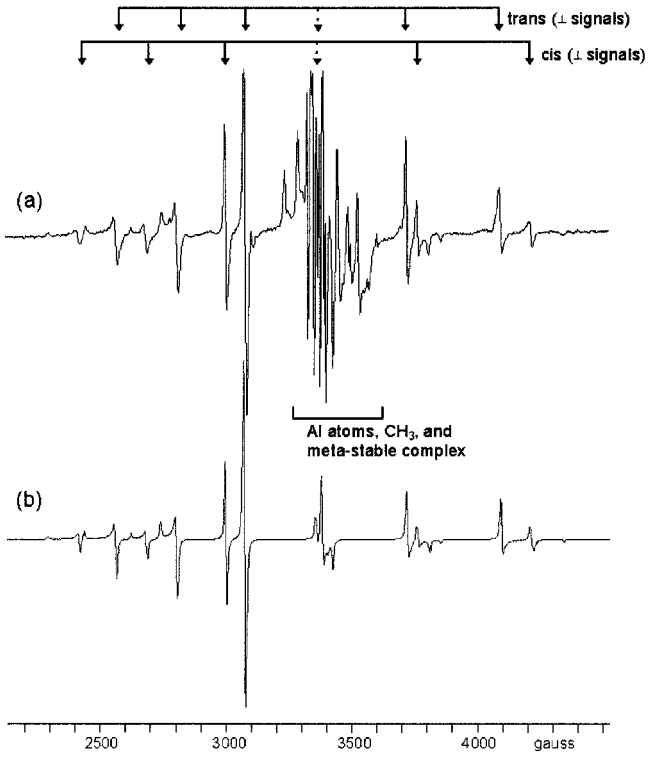

Figure 7. (a) ESR spectrum observed form the Al/DME(1%)/argon system. Two major sets of sextets were recognized and assigned to the insertion radicals $CH_3-Al-O-CH_3$ of the cis and trans configurations as indicated. (b) The simulated pattern based on the *g* and Al hfc tensors given in Table 1 and assumed abundance ratio of $^1/_3$ for the cis and trans conformers.

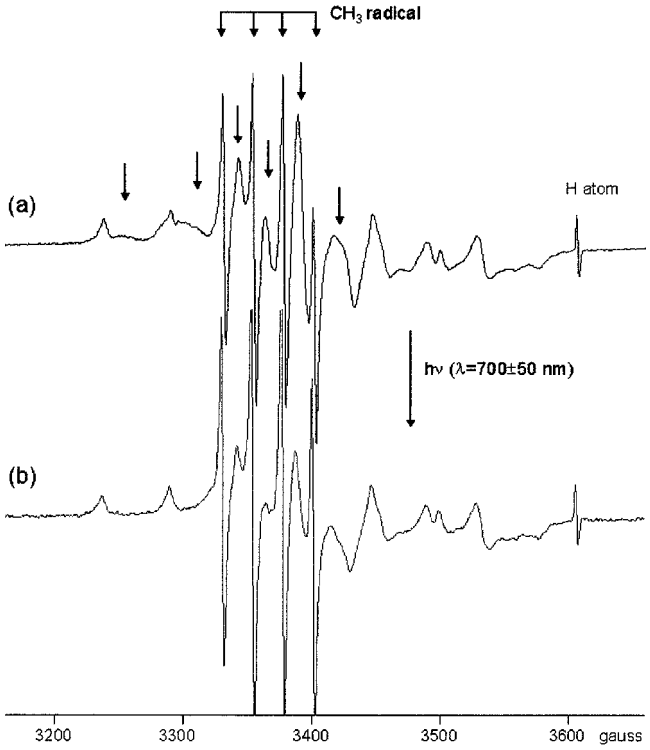

Figure 8. Central section of Figure 7a (under the bracket) observed (a) before and (b) after irradiation with red light ($\lambda = 700 \pm 50$ nm) for 20 min. The photoirradiation resulted in decrease of signals indicated by arrows and increase of the quartet due to methyl radicals.

carbon 2p orbitals. It is also revealed, in Figure 8, that irradiation with red light leads to generation of additional methyl radicals. It is thus indicated that methyl radicals are formed when, at

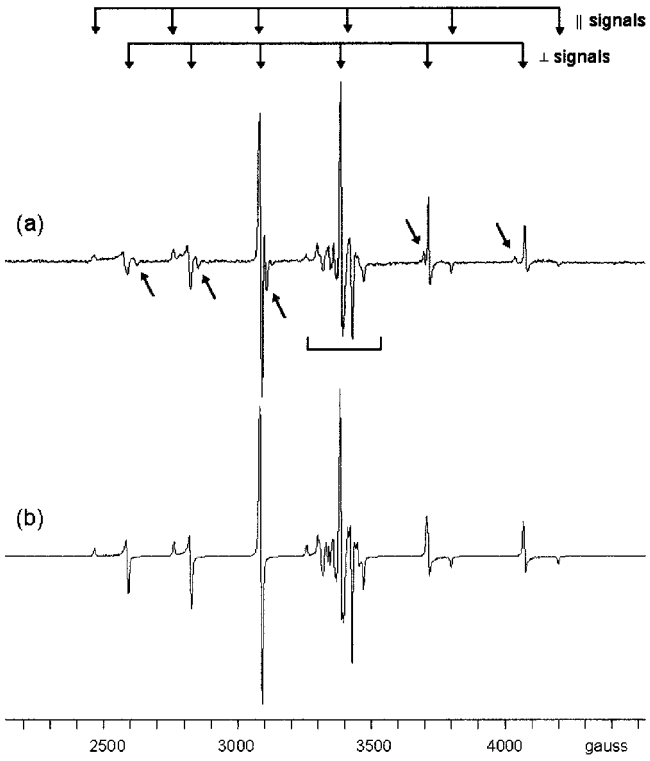

Figure 9. (a) ESR spectrum observed from the Al/DME(1%)/neon system. The spectral pattern due to the insertion radical Al−DME with an axially symmetric Al hfc tensor was recognized as indicated. The satellite (indicated by slant arrows) is due to insertion radicals complexed with the second DME molecule. (b) The simulated spectrum based on the *g* tensors and the Al hfc tensors given in Table 1 and the assumed abundance ratio of $^5/_3$ for the insertion radical and the intermediate dative complex (see text and Figure 10).

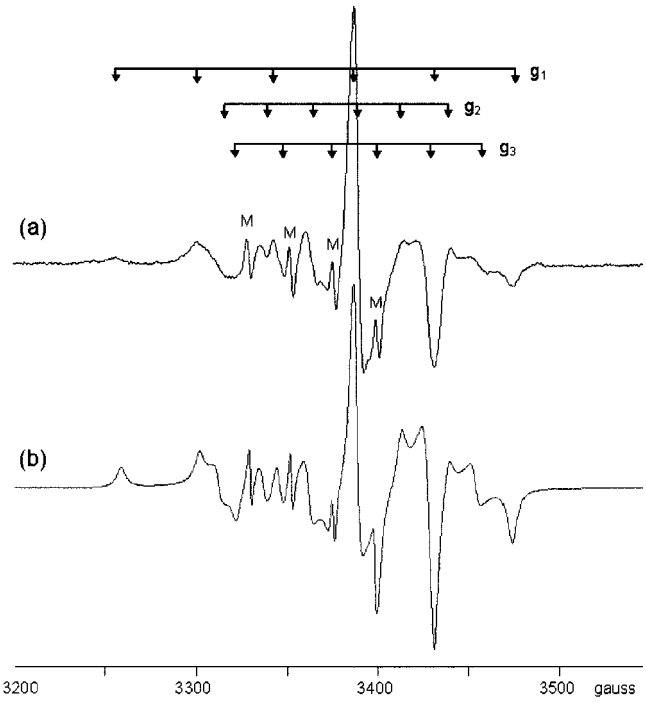

Figure 10. (a) Central section of Figure 9a observed in an expanded scale. The major pattern is ascribed to the intermediate dative complex $Al{:}O(CH_3)_2$; its *g* tensor and the Al hfc tensor were assigned as indicated. The letter M indicates the quartet due to methyl radicals. (b) The spectrum simulated based on the *g* and the Al hfc tensor of the intermediate dative complex given in Table 1. The signals due to methyl radicals (0.5%) are superposed as internal calibration.

stage D in Figure 2, the methyl group moves away from the reacting system instead of undergoing the three-electron bonding scheme with the lone pair electrons on the Al atom.

Figure 9a shows the ESR spectrum observed from the Al/DME(1%)/neon system. Unlike the previous situation in the argon matrix, only one dominant sextet is observed. The *g* tensor and the Al hfc tensor of this radical were found to be close to those of the trans radical observed in the argon matrix (see Table 1). It is thus concluded that, in a neon matrix, the barrier for the cis−trans conversion is lower, and only the most stable, trans-from is observed. A weaker satellite like sextet with a slightly smaller Al hfc tensor (indicated by slanted arrows) is ascribed to the insertion radical (of the trans form) datively complexed with the second DME molecule.

As stated earlier, no signals due to isolated Al atoms were observed in the Al/TMO(1−2%)/neon system. It is surmised that, in a softer neon matrix, all the Al atoms encounter a reacting partner supplied in an overwhelming excess. Figure 10a shows the central section of Figure 9a (indicated by the bracket) observed in an expanded scale. The signals due to isolated Al atoms are absent. The pattern consists of that due to methyl radicals, that of the fourth hf component of the insertion radical, and that of a third species having a small but highly anisotropic Al hf coupling tensor. The latter was assigned to the metastable dative complex (stage C in Figure 2) alluded to above. These signals were analyzed to yield the *g* tensor and the Al hfc tensor of orthorhombic symmetry as indicated and given in Table 1. Figure 10b is a computer-simulated pattern of the dative complex based on these tensors. In the simulation, the signals due to methyl radicals (5%) were superposed as they serve the purpose of internal calibration. Figure 9b shows the computer simulated pattern of the Al/DME/Neon system assuming the abundance ratio of $^5/_3$ for the insertion product and the meta-stable dative complex. Figure 11 shows the spectral change observed when the Al/DME(1%)/neon system was irradiated with red light ($\lambda = 700 \pm 50$ nm) for 20 min. In accord with the postulated reaction sequence, the irradiation resulted in a near total disappearance of the signals due to the dative complex and an increase of the signals of the insertion radical. Not unexpectedly, some additional methyl radicals were also produced in the process. The percentage increase of the insertion radicals (the main and the satellite combined) is just about what is predicted from the abundance ratio of $^5/_3$ for the insertion radical and the dative complex estimated in Figure 9.

Efforts to resolve the hf structure due to the methyl protons in the third Al hf component of the insertion radical was not successful. Figure 12 compares the third Al hf components observed from the Al/DME(1%)/neon and Al/DME(2%)/neon systems, respectively. They are shown in the integrated form instead. The dependency of the intensity of the satellite relative to the main peak upon the DME concentration is clearly revealed, and the presence of the second satellite is also indicated. The observed dependency is consistent with the postulate that these satellites are primary insertion radicals datively complexed with one or two additional DME molecules, respectively. The additional DME molecule(s) may datively interact with the Al center of the insertion radical in a head-on manner (a mode akin to stage C of Figure 2) or in a side-on manner (a mode akin to stage G of Figure 2). An MO study of the insertion radical complexed with one DME molecule indeed revealed a local energy minimum with the heat of complexation of 9 and 5 kcal/mol for the head-on mode and the side-on mode, respectively. The MO study also predicted a reduction of the Al hfc tensor (from that of the primary insertion radical of the trans form) by 40% for the head-on case and by 4% for the

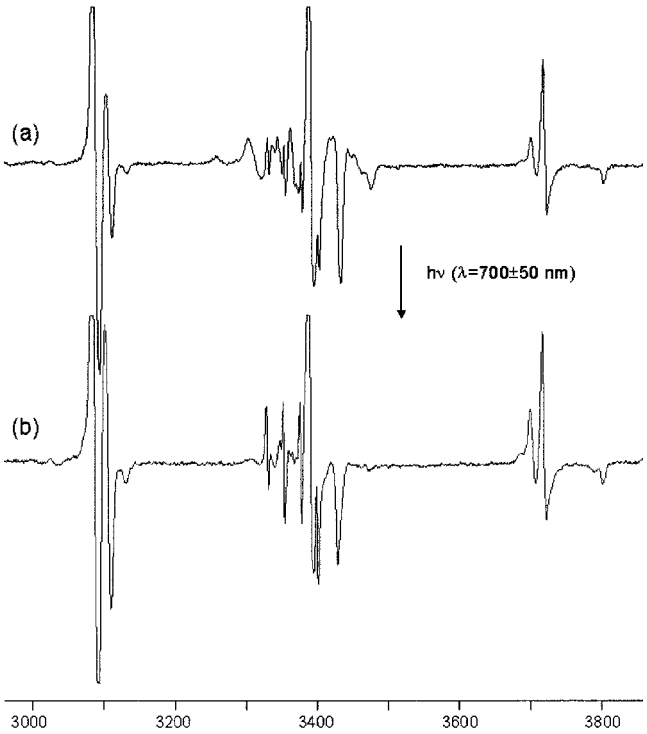

Figure 11. Middle section of the ESR spectrum of the Al/DME(1%)/neon system (encompassing the third to fifth hf components of the insertion radical) observed (a) before and (b) after irradiation with red light ($\lambda = 700 \pm 50$ nm) for 20 min. The irradiation resulted in a near total disappearance of the intermediate complex, and increase of the insertion radical.

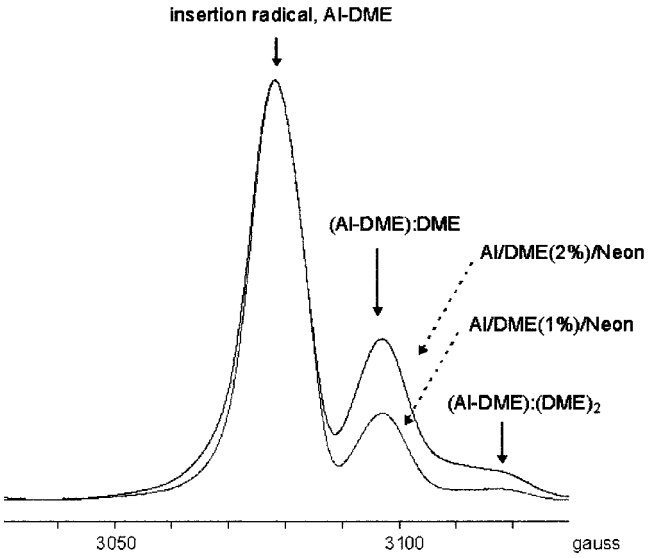

Figure 12. Third Al hf components observed from the Al/DME(2%)/neon and Al/DME(1%)/neon systems shown in the integrated form. The satellites are assigned to primary insertion radicals complexed with one and two additional DME molecules as indicated.

side-on case. The observed Al hfc tensor of the satellite is 4% smaller than that of the primary insertion radical. It is thus strongly suggested that the satellites are due to insertion radicals datively complexed with one or two DME molecule(s) in the side-on mode.

Summary and Concluding Remarks

The insertion process of the Al atom into the TMO (trimethylene oxide) molecule and that into the DME (dimethyl ether) molecule were examined by a semiempirical SCF molecular orbital method (AM1) and by matrix isolation ESR spectroscopy. The MO study has revealed that the process would occur in three steps. (1) The Al atom approaches the ethereal oxygen along the C_{2v} axis of the molecule driven by a facile overlap between the aluminum SOMO (the $3p_z$ orbital) and the LUMO of the molecule of A_1 symmetry. (2) As the Al−O bond is formed, one of the R−O bonds cleaves resulting in ring rupture in the case of TMO and detachment of the methyl radical in the case of DME. (3) The three-electron bonding interaction occurs between the unpaired electron of the alkyl terminus and the lone pair electrons on the Al atom, thus completing the process and transferring the unpaired electron back to the Al atom. The MO study has also revealed that the process would be entirely spontaneous for the Al/TMO system, but for the Al/DME system, there exists a barrier of ∼8 kcal/mol for the onset of the methyl group cleavage from the dative complex $Al{:}O(CH_3)_2$ formed in step (1). The MO study has also revealed that, in the Al/DME case, the insertion product $CH_3-Al-O-CH_3$ of the cis conformation is initially formed but it may readily convert to the more stable trans form.

The matrix isolation ESR study has revealed that the Al atom insertion into TMO does occur spontaneously. Well-resolved spectra of the expected insertion radical $\overline{CH_2-Al-O-CH_2-CH_2}$ were observed. In the case of DME, the ESR study revealed the presence of both the intermediate dative complex and the final insertion product in the as-prepared matrix. When the matrix was subsequently irradiated with red light ($\lambda = 700 \pm 50$ nm), the dative complex resumed the process and converted to the insertion product. The insertion radicals of both the cis and trans forms were observed in the argon system, but only the more stable trans radical was observed in the neon system.

As stated in the computation section, when the simulated adiabatic reaction for the Al atom and DME came to a halt at stage C in Figure 2, moving the Al atom slightly (∼0.1 Å) away from the symmetry axis resulted in resumption of the insertion process to the final product. Argon and neon matrixes in which Al atoms and TMO or DME molecules had been co-condensed appeared green in color. The effect of irradiation with red light observed for the Al/DME system is believed to be that of exciting the intermediate species vibrationally by warming the matrix.

That the entire process occurs spontaneously for the Al/TMO system while some, albeit small, activation is required for the Al/DME system is attributed to the ring strain of the TMO molecule. The MO result showed that the LUMO of TMO would be ∼0.33 eV lower than that of DME. In the TMO ring, the bonding orbitals would be less bonding due to the strain, and the antibonding system would be less antibonding allowing easier migration of the electron from the Al atom.

The Al hfc tensors determined for the various radicals observed in the present study are all (basically) axially symmetric (see Table 1). The principal elements of the tensor are thus given by $A_{||} = A_{iso} + 2A_{dip}$ and $A_{\perp} = A_{iso} - A_{dip}$, where A_{iso} is the isotropic component due to the spin density in the Al 3s orbital and A_{dip} is the anisotropic component due to the spin density in the Al 3p orbital.[19] Thus, for example, one obtains $A_{iso} = 336$ G and $A_{dip} = 20$ G for the insertion product Al−TMO in a neon matrix (cf. Table 1). These values are to be compared with $A^{\circ}_{iso} = 1400$ G computed for a unit spin density in the Al 3s orbital and $A^{\circ}_{dip} = 30$ G computed for a unit spin density in the Al 3p orbital.[20] Thus, as stated earlier, the unpaired

electron densities in the Al 3s and 3p orbitals of 0.24 and 0.67, respectively, were obtained.

Similar analyses of the Al hfc tensors determined for the Al−DME insertion radicals observed in argon matrixes yield $A_{iso} = 374$ G and $A_{dip} = 17$ G for the cis radical and $A_{iso} = 322$ G and $A_{dip} = 17$ G for the trans radical. In the ESR spectrum of Al−DME insertion radicals generated in adamantane at 77 K,[4] Chenier et al. observed the Al hf structure of $A_{iso} = 358$ G.[4] It is likely that the insertion radicals in the adamantane matrix are not only rotating but also undergoing rapid conversion between the cis and trans forms at 77 K.

As stated earlier, the hfc tensors of Al atoms isolated in rare gas matrixes had been analyzed by Ammeter et al.[15] The ESR spectra of the otherwise degenerate system ($3s^23p^1$) become observable owing to an axially symmetric lattice distortion. The unpaired electron thus resides in the nondegenerate 3p orbital. The hfc tensors have been determined as $A_{||} = +46.3$ G and $A_{\perp} = -35.3$ G for Al atoms in a neon matrix and $A_{||} = +47.7$ G and $A_{\perp} = -33.7$ G for those in an argon matrix. These values yield $A_{iso} = -8.1$ G and $A_{dip} = 27.2$ G in the neon case and $A_{iso} = -6.6$ G and $A_{dip} = 27.1$ G in the argon case. The small negative A_{iso}'s are due to spin polarization of filled s orbitals. The A_{dip} values are close to the computed "atomic value" of 30 G. As stated earlier, the MO study showed that the SOMO of the intermediate dative complex $Al{:}O(CH_3)_2$ consists of the Al 3p orbital and the carbon 2p orbitals. The signs of the hfc tensor elements cannot be determined from the spectrum. Let us assume, in line with the tensors concluded for isolated Al atoms, $A_{||} = +43.0$ G and $A_{\perp} = -25.9$ G for the dative complex. One then obtains $A_{iso} = -2.9$ G and $A_{dip} = 23$ G. The A_{dip} value is significantly less than that of isolated Al atoms and is consistent with the predicted migration of the unpaired electron into the DME moiety.

References and Notes

(1) Hauge, R. H.; Kauffman, J. W.; Margrave, J. L. *J. Am. Chem. Soc.* **1980**, *102*, 6005.

(2) Knight, L. B. Jr.; Gregory, B.; Cleveland, J.; Arrington, C. A. *Chem. Phys. Lett.* **1993**, *204*, 168.

(3) Howard, J. A.; Joly, H. A.; Edwards, P. P.; Singer, R. J.; Logan, D. E. *J. Am. Chem. Soc.* **1992**, *114*, 474.

(4) Chenier, J. H. B.; Howard, J. A.; Joly, H. A.; LeDuc, M.; Mile, B. *J. Chem. Soc., Faraday Trans.* **1990**, *86*, 3321.

(5) Köppe, R.; Kasai, P. H. *J. Am. Chem. Soc.* **1996**, *118*, 135.

(6) Sakai, S. *J. Phys. Chem.* **1992**, *96*, 8369.

(7) Sakai, S. *J. Phys. Chem.* **1993**, *97*, 8917.

(8) Fängström, T.; Mirrander, A.; Ediksson, L. A.; Lunell, S. *J. Chem. Soc., Faraday Trans.* **1998**, *94*, 777.

(9) Kasai, P. H. *J. Phys. Chem A* **2000**, *104*, 4514.

(10) Kasai, P. H. *Acc. Chem. Res.* **1971**, *4*, 329.

(11) *HyperChem 5.1*; Hypercube, Inc.: Gainesville, FL, 1998.

(12) Kasai, P. H. *J. Am. Chem. Soc.* **1972**, *94*, 5950.

(13) *Absoft Pro Fortran 5.0*; Absoft Corporation: Rochester Hills, MI, 1998.

(14) Kasai, P. H. *J. Am. Chem. Soc.* **1990**, *112*, 4313.

(15) Ammeter, J. H.; Schlosnagle, D. C. *J. Chem. Phys.* **1973**, *59*, 4784. For ESR spectra of Al atoms in rare gas matrixes, see: Knight, L. B., Jr.; Weltner, W., Jr. *J. Chem Phys.* **1971**, *55*, 5066.

(16) Kasai, P. H.; McLeod, D., Jr. *Faraday Discuss. Symp. 14, Chem Soc.* **1980**, 65.

(17) Pryce, M. H. L. *Proc. Phys. Soc., London Sect. A.* **1950**, *63*, 25.

(18) Moore, C. E. *Natl. Stand. Ref. Data Ser. (U.S. Natl. Bur. Stand.)* **1971**, 35.

(19) See, for example: Smith, W. V.; Sorokin, P. P.; Gelles, I. L.; Lasher, G. J. *Phys. Rev.* **1959**, *115*. 1546.

(20) Morton, J. R.; Preston, K. F. *Magn. Reson.* **1978**, *30*, 577. <<